Materials Advances

ROYAL SOCIETY OF CHEMISTRY

PAPER

View Article Online
View Journal | View Issue

Cite this: *Mater. Adv.*, 2025, 6, 378

Generic strategy for the synthesis of highly specific Au/MIP nanozymes and their application in homogeneous assays†

Shaemaa Hadi Abdulsada,[ab] Alvaro Garcia Cruz, *[a] Christopher Zaleski,[a] Elena Piletska,[a] Damla Ulker,[a] Stanislav Piletsky[c] and Sergey A. Piletsky[a]

Enzymes are highly complex nanomachines produced by cells with the ability to catalyse diverse chemical reactions. Their applications in biotechnology and molecular diagnostics are widespread. However, most enzymes suffer from poor operational and storage stability and high manufacturing costs. Identifying suitable enzyme for particular substrates of practical importance is often challenging. These limitations are driving the search for synthetic alternatives – nanoparticles with catalytic properties that can mimic enzymatic reactions (nanozymes). A broad variety of organic and inorganic nanoparticles have been developed with catalytic power matching that of natural enzymes. Unfortunately, developing nanozymes with substrate/ligand specificity akin to that of enzymes and antibodies has proven challenging. Here we report a novel generic strategy for the synthesis of highly specific nanozymes mimicking peroxidase based on MIP nanoparticles with gold cores, prepared by a Fenton-like reaction. Synthesis of MIP shells was achieved by localised radical polymerization of monomer mixture triggered by hydroxyl radicals produced by hydrogen peroxide decomposed on the gold surface. The products of this reaction are highly specific and robust composite Au/MIP nanoparticles (Au/MIP nanozymes) with integrated biorecognition and catalytic properties. In this work we also explore the use of synthesised Au/MIP nanozymes in oxidation of BPR by hydrogen peroxide for colorimetric detection of template analytes such as amphetamine. The developed assay allowed the detection of corresponding analytes at nanomolar concentrations in complex biological matrices. The assay was robust and easy to perform with minimal operational steps. These findings hold great promise for developing a new form of homogeneous, completely abiotic, highly sensitive, highly specific user-friendly assays for *in vitro* diagnostics.

Received 10th September 2024,
Accepted 14th November 2024

DOI: 10.1039/d4ma00917g

rsc.li/materials-advances

1. Introduction

Developing nanozymes (nanoparticles with enzyme-mimicking catalytic properties) holds tremendous value for diagnostics due to their ability to overcome the limitations of natural enzymes, such as susceptibility to denaturation, lack of substrate selectivity, and the expense and labour-intensive nature of their preparation.[1,2] The use of nanoparticles as nanozymes catalysing many different reactions has been well documented.[3–6] Nanozymes mimicking horseradish peroxidase (HRP) are particularly useful due to the widespread applications of this enzyme in assays and sensors.[4–6] Some good examples of nanozymes mimicking peroxidase are metal and metal oxides nanoparticles employed for the detection of glucose in colorimetric reaction with H_2O_2 and 3,3′,5,5′-tetramethylbenzidine (TMB) or 2,2′-azinobis (3-ethylbenzothiazoline-6-sulphonic acid)-diammonium salt (ABTS).[7–9] The role of HRP or corresponding nanozyme mimics in assays and sensors lies in providing signal amplification for detecting low concentrations of analytes. Possessing catalytic function, however, is insufficient for effective use of nanozymes in assays and sensors since the ideal material for such applications would require integrated catalytic and recognition functions. To achieve this, nanozymes are often functionalised with antibodies or DNA.[10–12] This unfortunately is not an ideal solution since antibodies and DNA have low intrinsic stability, especially in non-physiological conditions.

One potential solution to these problems involves the use of molecular imprinting to create binding sites on the nanozyme's surface, thereby adding specific recognition to the innate catalytic power of nanoparticles.[13–16] Molecularly imprinted

[a] *University of Leicester, Chemistry Department, University Rd, Leicester LE1 7RH, UK. E-mail: agc14@leicester.ac.uk*
[b] *Mustansiriyah University, College of Science, Chemistry Department, 10047 Baghdad, Iraq*
[c] *Memorial Sloan Kettering Cancer Center, 1275 York Avenue, ZRC-13S New York, NY 10065, USA*

† Electronic supplementary information (ESI) available. See DOI: https://doi.org/10.1039/d4ma00917g

polymers (MIPs) offer the potential to provide the same level of specificity and selectivity as biological receptors, while also being affordable, durable, and capable of indefinite storage without requiring special environmental conditions.[17] In contrast to natural receptors, MIPs can tolerate a much wider range of temperatures and pH values.[18,19] Their properties are tuneable and customizable, which renders them ideal for use in assays and sensors.[19] Another advantage is that MIPs can be synthesized using a generic, 'standard' protocol which can be applied to imprint a diverse range of small molecules, peptides, and proteins.[20,21] Iron oxide and especially gold nanoparticles have previously been demonstrated to be able to serve as alternatives to HRP by generating a colorimetric signal in assays.[22,23]

Previously, nanozymes based on Fe_3O_4, CeO_2, and gold nanoparticles imprinted with dyes capable of catalyzing their oxidation were reported.[15] However, a significant challenge with this approach was that the dye itself acted as both the target molecule and the substrate, making it difficult to independently evaluate the nanozymes' recognition capabilities and catalytic activity. Additionally, both the iron oxide particles used as controls and the nanozymes demonstrated varying levels of catalytic activity, which facilitated dye oxidation. The limitations of these nanozymes were likely due to the aggregation of iron oxide particles caused by crosslinking during the synthesis process, which resulted in nanoparticles with poorly defined structures. As a result, both the molecularly imprinted (MIP) and non-imprinted (NIP) iron oxide nanoparticles displayed catalytic activity, complicating the evaluation of the imprinting process and making it difficult to differentiate the material's specific catalytic effects. This issue also led to cross-reactivity in both MIPs and NIPs, likely stemming from the uncontrolled formation of the polymer shell and inconsistent particle sizes during chemical polymerization in solution. To address these challenges, we employed solid-phase synthesis as an alternative approach.[20,21]

In the past, we have successfully developed MIP-coated iron oxide nanoparticles for heterogeneous assays.[21,24,25] These iron oxide nanoparticles played a crucial role in amplifying the signal generated by the specific binding of MIPs to the immobilized target. The intensity of colour developed in the catalytic reaction involving H_2O_2 and TMB was directly proportional to the analyte's concentration. Nevertheless, challenges emerged when employing iron oxide as a nanozyme, primarily due to persistent aggregation phenomena observed within such systems and the relatively modest catalytic effect displayed by iron oxide in this reaction. Also, we have previously described the use of iron oxide nanoparticles with intrinsic peroxidase-like activity in the presence of hydrogen peroxide for the development of heterogeneous colorimetric test for vancomycin.[24] These particles possessed a core–shell structure, with an imprinted polymer shell surrounding the Fe_3O_4 core. The assay was based on free vancomycin and vancomycin immobilized on the microtiter plate surface competing in binding to Fe_3O_4-MIPs. Upon addition of Fe_3O_4-MIPs and vancomycin, the extent of nanoparticles bound to the well surface was found to be dependent on the amount of free vancomycin in solution (by measuring the peroxidase activity) after incubation and washing to remove unbound Fe_3O_4-MIPs. The peroxidase activity was determined by addition of standard colorimetric substrate 3,3′,5,5′-tetramethylbenzidine (TMB) for ELISA and hydrogen peroxide. Although the developed assay benefited from the robustness of the components involved, the procedure still required multiple steps including a washing step, which limited its efficiency. In addition, the immobilisation of the template onto microplate wells is tedious and led to experimental errors.

Alternatively, gold nanoparticles can serve as a superior alternative to metal oxide catalysts.[7] Gold-based nanozymes exhibit the ability to catalyse various reactions (albeit non-specifically).[26] They particularly excel as peroxidase mimics, finding application in a multitude of assays and sensor platforms.[27] However, functionalizing gold nanoparticles with MIPs is not a straightforward task. Ideally, the polymerization reaction should be confined to the surface of the nanoparticles, obviating the complex process of separating MIP-coated gold from the polymers formed in solution. The process of polymer grafting can capitalize on the fact that many well-known nanomaterials exhibit catalytic activity in polymerization reactions, including nanoparticles made of cerium oxide, gold, platinum, palladium, V_2O_5, Fe_3O_4, and graphene oxide.[28] This unique attribute enables polymerization to occur on the surface of catalytic nanoparticles without the need for additional initiators.[29] The present solid-phase synthesis method enables precise control over particle size and catalytic properties, resulting in well-defined, individual nanoparticles. Crucially, the gold nanozymes exhibit distinct recognition and catalytic behaviours, with no cross-reactivity observed, addressing the limitations of earlier methods. Additionally, this approach can be effectively applied in biological matrices, making it suitable for forensic applications. This represents a significant advancement in the development of nanozymes for specific target detection in complex environments.

This study introduces solid-phase synthesis as a novel approach for nanozyme assembly, offering significant advancements. Additionally, it presents a colorimetric assay specifically designed for forensic applications. We propose the development of gold-based nanozyme particles specifically tailored for small target molecules like amphetamine, mimicking the recognition properties of antibodies with the catalytic activity of enzymes. Unlike previous reports, these gold nanozymes demonstrate target-specific recognition through an ''actuation'' mechanism, where binding to the target molecule induces structural changes similar to antibody–antigen interactions. This binding also activates the nanozymes' catalytic properties, mimicking the induced-fit mechanism seen in enzymes. These properties are applied in a colorimetric assay using dyes as reporting agents. This article outlines the solid-phase synthesis process of MIP-coated gold nanoparticles imprinted with amphetamine. The procedure relies on the Fenton-like catalytic activity of gold nanoparticles, which can effectively catalyse hydrogen peroxide disproportionation. The formation of hydroxyl radicals on the gold surface initiates a confined polymerization reaction onto the nanoparticle surface. This reaction results in the

creation of highly specific and durable composite Au/MIP nanozymes, possessing both integrated biorecognition and catalytic properties. Catalytic properties of the synthesized Au/MIP nanozymes were investigated and exploited in the oxidation of BPR by hydrogen peroxide for the colorimetric detection of amphetamine. The choice of amphetamine as the target analyte illustrates the efficiency of the developed protocol in forensic applications.

2. Results and discussion

2.1 Synthesis and characterization of Au/MIP nanozymes

Nanozymes were prepared by solid-phase synthesis of molecularly imprinted polymers (MIPs) using a Fenton-like reaction (Scheme S1, ESI†). Typically, this reaction involves the catalytic decomposition of hydrogen peroxide in the presence of ferrous ions. Similarly, gold catalysts operate in the same manner. The polymerisation mechanism take place *via* a free-radical polymerization (Scheme 1). Gold nanoparticles catalyse the decomposition of hydrogen peroxide into hydroxyl radicals (•OH). These radicals react with acrylamide monomers (AAm), initiating polymerization. The polymerization process continues, forming a polyacrylamide matrix decorated with gold nanoparticles. Additionally, acrylamide monomers may contribute to regenerating the gold catalyst by serving as reducing agents. Also, hydrogen peroxide serves as both the oxidizing and reducing agent, decomposing into O_2 as a byproduct. As result MIP decorated with AuNPs are obtained. As previously described, gold nanoparticles are considered a particularly promising alternative to iron or iron oxide in a catalytic Fenton process. They have been observed to catalyse the formation of hydroxyl radicals from hydrogen peroxide with much higher efficiency and higher turnover than iron and iron oxide nanoparticles.[30,31] The lifetime of HO• is very short (20 ns) and HO• can be quenched by the solvent with rapid kinetics (1–40 × 10^8 nM^{-1} s^{-1}).[32] Using gold nanoparticles as a catalyst strategically confines the polymerization reaction to the surface of the gold nanoparticles, yielding core–shell nanoparticles distinguished by precise control of the thickness of the polymer layer.

Moreover, polymer specificity arises from conducting the polymerization reaction in the presence of template molecules immobilized on a solid surface. Consequently, the generated nanozyme, after removal, contains recognition sites specific to the target molecule. The solid phase approach to molecular imprinting has proven to be an effective tool for producing "monoclonal" MIPs with superior affinity and specificity.[33–36] Incorporating a gold core into hybrid nanoparticles not only facilitates efficient Fenton catalysis but also triggers catalytic reactions analogous and tailored to enzymatic processes, such as catalase or peroxidase. (Fig. 1).

Au/MIP nanoparticles (Au/MIP nanozymes) were prepared as described in the Methods section, using commercial gold nanoparticles with size 5–100 nm. Control nanoparticles (Au/NIP nanozymes) were synthesized in the same manner but in the absence of target molecules. The chemical composition of the nanozymes was characterized through FTIR analysis,

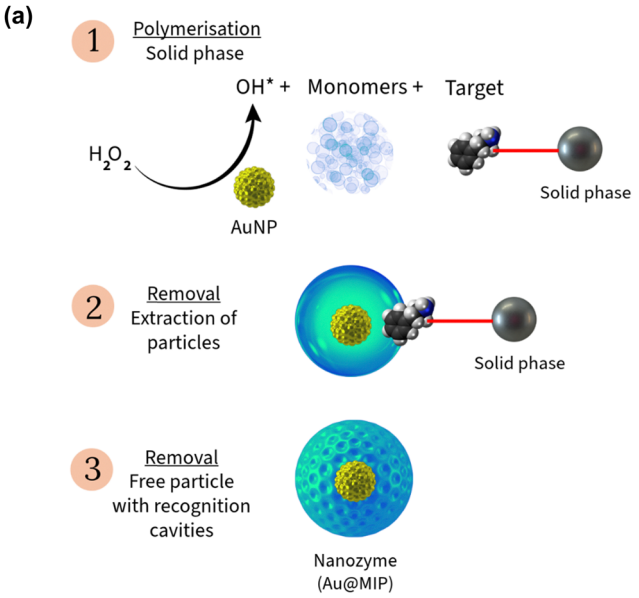

(b)

1) $Au^0 + H_2O_2 \rightarrow Au^{3+} + 2{\bullet}OH$
2) $\bullet OH + AAm \rightarrow \bullet AAm + H_2O$
3) $\bullet AAm + AAm \rightarrow \bullet AAm\text{-}AAm$
4) $Au^{3+} + \bullet AAm\text{-}AAm \rightarrow Au\text{-}AAm\text{-}AAm$
5) $Au^{3+} + H_2O_2 \rightarrow Au^{0+}{}^{\bullet}OOH + H^+$

Scheme 1 (a) Polymerisation steps: radical generation at the gold surface and polymerisation of acrylamide moniomers at target molecule immobilised at the solid phase. (b) Thermal removal of particles using solvent washes. (c) Nanozymes particles are obtained in the extracted solution. (b) Polymerisation mechanism: (1) initiation: hydrogen peroxide (H_2O_2) is decompased by gold catalyst to into hydroxyl radicals (•OH). (2) Chain initiation: the hydroxyl radicals react with acrylamide (AAm) to generate acrylamide radicals (•AAm). (3) Chain propagation: acrylamide radicals propagate the polymerization by reacting with more acrylamide monomers. (4) This process continues, forming polyacrylamide chains aggregating to form Au@MIP. (5) Hydrogen peroxide acts as both an oxidizing and reducing agent, generating radicals and spliting water into O_2 as a byproduct.

confirming the presence of a polyacrylamide shell (Fig. S1, ESI†). Representative transmission electron microscopy (TEM) images of the core–shell particles produced in this work are shown in Fig. 2. Dynamic light scattering (DLS) results show similar size for the Au/MIP and Au/NIP nanozymes (124.5 ± 1.8 nm, PDI = 0.112, and 107.9 ± 2.3 nm, PDI = 0.163, correspondingly). These low PDI values suggest that the nanoparticles in both samples were relatively uniform. TEM images and DLS data presented indicated a significant variation in size of synthesised Au/MIP nanozymes, varying from 98.4 for 5 nm Au core to 726 nm for 100 nm Au core nanoparticles. The primary reason for this discrepancy is that DLS measures the hydrodynamic size of gold particles in solution, where they tend to aggregate, and the measurement is based on light scattering, which is less precise than electron microscopy. In contrast, TEM involves sample preparation methods such as electric discharge and sonication, which disperse the particles,

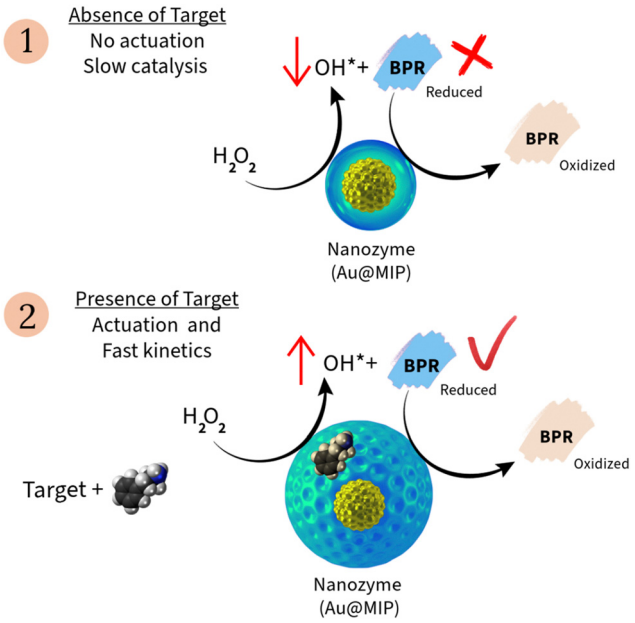

Fig. 1 Schematic representation of the colorimetric assay principles: (1) in the absence of the target molecule, the polymeric shell of the nanozymes hinders the production of radicals, resulting in slow oxidation of the dye. Consequently, no significant changes in absorbance are measured. (2) When the nanozyme recognizes the target, actuation is triggered, leading to swelling of the polymer. This results in rapid kinetics and high catalytic activity, allowing for the oxidation of the target, which is then measured by absorbance.

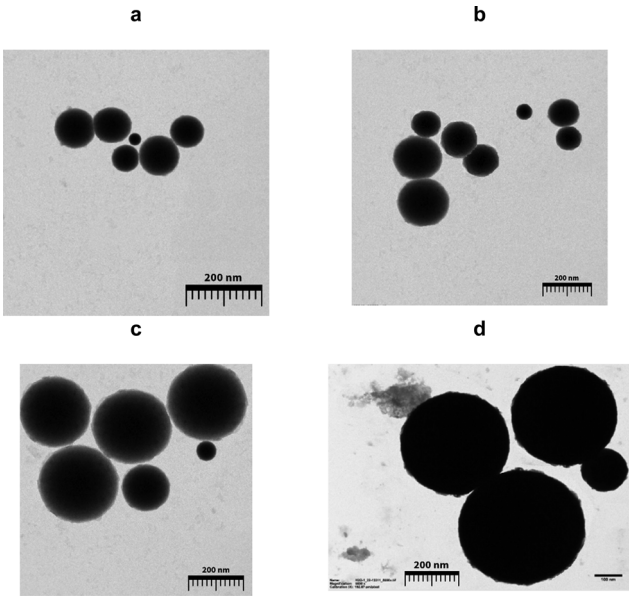

Fig. 2 TEM images depict (a) Au/MIP1, (b) Au/MIP2, (c) Au/MIP3, and (d) Au/MIP4 at a 200 nm scale. These images showcase Au/MIP nanoparticles where the size of AuNPs was systematically varied to 5 nm, 20 nm, 50 nm, and 100 nm, respectively.

allowing for the identification of individual particles on dry copper grids. TEM also provides nanometre scale resolution, offering a more accurate measurement of particle size.

Remarkably, each Au/MIP nanozyme features a gold core embedded within a polymeric shell (Fig. 2). Smaller Au nanoparticles appear to be more conducive to generating consistent core–shell structures, unlike larger Au nanoparticles where the polymerization reaction is not confined solely to the gold surface. The catalytic properties of synthesised Au/MIP nanozymes were assessed *via* a colorimetric assay with BRP (see Materials and method section). Overall there is clear connection between the size of gold core and the catalytic activity of Au/MIP nanozymes (Table 1).

2.2 Assay principles

The colorimetric assay developed in this work offers an alternative to the traditional enzyme-linked immunosorbent assay (ELISA). In this context, the catalytic activity of the Au/MIP nanozyme is modulated by its binding interaction with the specific target molecule (amphetamine in this case). The mechanism underlying these nanozymes is rooted in the well-established Fenton-like reaction, and involves two key components.[37] First, the gold cores of the nanozyme catalyse the decomposition of hydrogen peroxide (H_2O_2) into hydroxyl radicals ($HO^{\bullet}$) onto their surfaces that can be detected *via* colorimetric reactions (Fig. 1). The second component of the assay relates to the analyte binding to the MIP, which triggers structural changes in the polymer, in a way mimicking the "induced fit" actions characteristic of enzymes and natural receptors. Specifically, this involves swelling of the nanozyme shell, which exposes sections of the gold core available for catalysis.

The combined actions of these two components produces analyte-specific enhancement of the catalytic activity of the Au/MIP nanozymes in the Fenton-like reaction with hydrogen peroxide and the dye BPR. This effect, mimics the peroxidase-like activity commonly observed in colorimetric assays. A decrease in BRP absorbance correlates with the concentration of amphetamine in the sample. Overall, this mechanism allows specific detection of the target molecules in complex biological samples through a homogeneous colorimetric assay, providing a sensitive and specific diagnostic tool. This innovative approach combines the catalytic properties of gold nanoparticles with the specificity of MIPs, offering a promising avenue for the development of homogeneous diagnostic assays with enhanced resilience and simplicity compared to traditional enzyme-based assays. Herein, an assay specific for amphetamine detection in biological fluids was developed and numerous factors have been optimized, including incubation time, BPR, nanozyme, peroxide, and analyte concentration.

The actuation mechanism relies on analyte recognition, which triggers conformational changes in nanozyme, leading to swelling and an increase in volume and surface area. This mechanism was previously demonstrated using dynamic light scattering (DLS) measurements.[20] In this study, the swelling effect was observed exclusively in the presence of the specific target, resulting in a 20% increase in volume, while no significant changes were noted with other drugs. This effect increased in previous report sensor signal response. This mechanism is

Table 1 Parameters of synthetised Au/MIP nanozymes and their assay performance. Assay conditions: each well contained 10 μL of the nanozyme (0.4 mg mL^{-1}), 135 μL of 10 nM BPR in PBS (5 mM, pH 7), 135 μL of H_2O_2 (50% w/v) and 20 μL of amphetamine

MIP particle	Diameter of Au core[a] (nm)	Diameter of Au/MIP nanozyme particles[b] (nm)	K_m (mM)	V_{max} (nM s^{-1})	LOD (nM)	Linear range (nM)
MIP1	5	98.4 ± 2.4	4.0	1.5×10^{-4}	0.17	0.6–40
MIP2	20	124.5 ± 1.8	3.8	1.0×10^{-4}	0.23	0.6–40
MIP3	50	324.2 ± 7.3	5.5	7.0×10^{-5}	0.46	2.0–40
MIP4	100	726.9 ± 13.6	4.0	5.5×10^{-5}	0.52	10–40
NIP	5	89.01 ± 3.1	1.0	5.0×10^{-5}	No response to the target	No response to the target

[a] TEM measurements. [b] DLS measurements.

akin to the "induced fit" observed in enzymes.[38] To illustrate the induced fit phenomena observed for developed nanozymes, their hydrodynamic size was measured in the presence of various targets using DLS. Thus Au/MIP nanozymes in solution displayed a size of 98.4 ± 1.5 nm (PDI, 0.130). Upon exposure to amphetamine, the Au/MIP nanozymes swelled, increasing in size by ~51% (Fig. S2, ESI†) confirming the amphetamine recognition by the Au/MIP nanozyme. Conversely, in response to the same concentration of paracetamol the size of the Au/MIP nanozymes showed negligeable size change (~4%). This outcome highlights that specific actuation exclusively occurs in the presence of the target analyte, as depicted in Fig. S2 (ESI†). The control experiments using a control Au/NIP (non-imprinted polymer, NIP) do not show any significant change (<2.6%). In addition, AuMIP's selectivity towards amphetamine was confirmed using localized surface plasmon resonance (LSPR). The nanozyme's LSPR response is sensitive to changes in polymer conformation due to the presence of gold nanoparticles. The binding of the target molecule induces conformational changes in the AuMIP polymer, which alters the local refractive index and, consequently, the plasmon resonance. Significant changes in the plasmon resonance of AuMIP (91%) were observed in the presence of amphetamine, as shown in Fig. S3 (ESI†). In contrast, AuMIP exhibited no significant interaction with paracetamol, confirming the specificity of amphetamine recognition.

2.3 Assay optimization

To optimize the colorimetric assay format in a 96-well microplate, firstly the BPR concentration was fine-tuned as illustrated in Fig. S4 (ESI†). The linear working range of the new assay was found to be 0.1 nM–40 nM (R^2 = 0.992), with the optimal BPR concentration found to be 10 nM. The catalytic activity of gold nanoparticles shows strong pH dependency, which can shift from peroxidase-like activity at pH values between 3.5 and 4.0, to catalase and peroxidase-like activity at neutral pH.[39] For this reason, all experiments with Au/MIP nanozymes were performed at neutral pH. Spectrometric measurements in kinetic mode revealed that BPR oxidation exhibited a notably faster rate at pH 7.0 than at other pH values, as indicated by the reaction rate (−0.1 pM s^{-1}) as shown in Fig. S5 and Table S2 (ESI†). Moreover, the optimal assay activity was attained at 0.4 mg mL^{-1} Au/MIP nanozyme (reaction rate, 0.06 pM s^{-1}). Notably, at high Au/NIP nanozymes concentrations, the catalytic activity decreased, possibly due to aggregation phenomena (Fig. S6 and Table S3, ESI†).

Subsequently, the optimal concentration of nanozymes was used to refine the hydrogen peroxide concentration, as depicted in Fig. S7 (ESI†). The reaction rate was found to depend on peroxide concentration, both with and without the presence of amphetamine. Furthermore, the reaction rate increased proportionally with amphetamine concentration until reaching its maximum velocity (V_{max}) at 14.7 mM H_2O_2. In the presence of amphetamine, the Michaelis–Menten constant (K_m) was lower (4.0 mM) compared to its absence (6.0 mM). This indicates that amphetamine enhances the reaction rate, as shown in Table S4 (ESI†). Accordingly, the kinetic study revealed a clear effect of amphetamine on BPR oxidation catalysed by Au/NIP nanozymes, as depicted in Fig. S8 and detailed in Table S5 (ESI†). Also, the catalytic activity dependency on amphetamine concentration can be observed on the UV-vis spectra of the assay, where it can be seen that absorbance decreases with increasing concentrations of amphetamine (Fig. S9, ESI†). Also, MIP1 and MIP2 exhibit higher catalytic activity compared to MIP3 and MIP4 (Fig. S10 and S11, ESI†). This difference is attributed to the size of the gold nanoparticles; smaller nanoparticles offer a larger surface area, leading to a higher reaction rate.

The linear range was found to be between 0.6 and 40 nM, under these conditions, as demonstrated in Fig. 3. Importantly, the detection range of the assay falls within a clinically relevant range for forensic applications. An amphetamine concentration ranging from 20 to 100 ng mL^{-1} (equivalent to 0.148 nM to 0.74 nM) in urine is considered acceptable and falls within the therapeutic range.[40] Conversely, concentrations exceeding 100 ng mL^{-1} (0.74 nM) in urine may indicate potential drug abuse and extremely high levels exceeding 2500 ng mL^{-1} (18.5 nM) can be toxic and potentially fatal. In contrast, concentrations surpassing 100 ng mL^{-1} (0.74 nM) in urine may suggest possible drug abuse, while exceptionally elevated levels exceeding 2500 ng mL^{-1} (18.5 nM) can be life-threatening and toxic.[41] The assay specificity was analysed by comparing responses of Au/MIP and Au/NIP nanozymes (Fig. 3 and Fig. S12, ESI†). Therefore, no noticeable response to amphetamine was detected for Au/NIP nanozymes. A fold change of 500 was found in the binding affinity towards the target between MIP and NIP, indicating a significantly greater specificity and efficiency of the MIP in recognizing and binding to the target molecule.

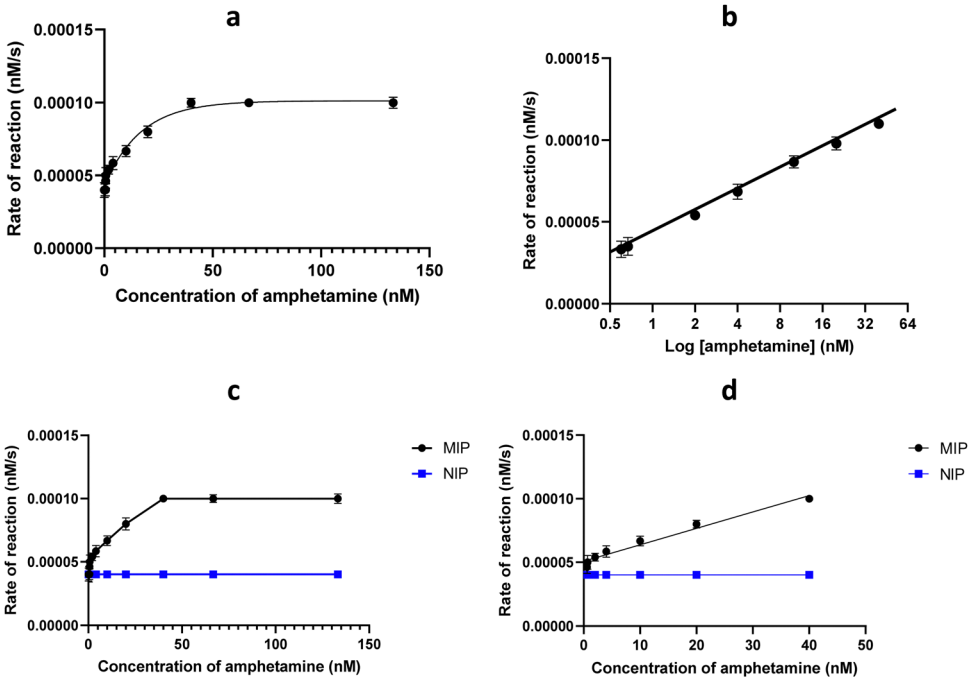

Fig. 3 The relation between amphetamine concentration and BPR rate of reaction. (a) Amphetamine concentration range 0–133 nM; (b) amphetamine concentration range 0–40 nM. Assay response to amphetamine using Au/MIP and Au/NIP nanozymes. (c) Amphetamine concentration range 0–133 nM; (d) amphetamine concentration range 0–40 nM. Assay conditions: each well contained 10 μL of the Au/MIP nanozyme (0.4 mg mL^{-1}), 135 μL of 10 nM BPR in PBS (5 mM, pH 7.0), 135 μL of H_2O_2 (50% w/v) and 20 μL of amphetamine solution (0, 0.3, 0.53, 0.6, 1, 2, 4, 10, 20, 40, 66.7, and 133 nM).

This demonstrates the effectiveness of the imprinting process. The imprinting factor was reported as suggested. The lack of catalytic activity observed in the non-imprinted polymer (NIP) primarily stems from the polymer shell shielding the catalytic surface of the gold nanoparticles, preventing any actuation (no swelling). This is due to the absence of recognition cavities. Consequently, when the NIP is exposed to the target, it fails to exhibit any catalytic response. Additionally, the imprinting factor indicates that the NIP control lacks significant catalytic activity. This compelling result proves the high specificity of the developed assay for a corresponding target.

Once the working conditions of the assay were established, efforts were directed towards optimizing the size of the gold core and the thickness of the polymer shell for the corresponding Au/MIP nanozymes. A comprehensive summary of the parameters that were fine-tuned for the synthesized nanozymes and assay performance is presented in Table 1. This resulted in the creation of 4 different MIP samples with particle sizes ranging from 100 to 627 nm, as depicted in Fig. 2. Our findings indicated that MIP1 and MIP2, with gold cores of diameter 5 nm and 20 nm respectively, exhibited the highest reaction rates in the oxidation of the BPR dye, as well as the highest response to amphetamine. Variations in gold concentration or polymerization time had very little impact on assay performance. The assay exhibited its highest response to amphetamine for smaller particles with a thinner layer of the polymeric shell (Fig. S13, ESI†). The assay selectivity was assessed for other drugs such as paracetamol, morphine, and cocaine. As depicted in Fig. 4, practically no cross-reactivity was observed for interfering molecules, demonstrating the excellent selectivity of Au/MIP nanozymes for a corresponding target.

Commonly, colorimetric ELISA assays often suffer from matrix effects and interference when used with biological samples due to the complex nature of these matrices. Biological samples, like blood or urine, contain cells, proteins, enzymes, small molecules such as urea, creatinine, electrolytes and other compounds that can non-specifically bind to the assay components or interfere with the signal generation. Also, biological samples can further complicate the detection by affecting enzyme activity or antibody binding. These interactions can alter the assay's sensitivity and specificity, leading to false positives or negatives.[42] To overcome these issues, the nanozymes present a potential solution to these issues, offering high specificity for the target molecule by creating recognition sites tailored to the analyte, thus reducing non-specific interactions. Additionally, nanozymes, which mimic enzyme activity, provide more controlled catalytic properties, which enhance the assay's selectivity. As result nanozymes can significantly minimize interference from biological matrices, making them more suitable for complex sample analysis in comparison to traditional ELISA. To demonstrate potential applications, the nanozymes assay was employed to detect amphetamine levels in both urine and plasma. The assay remains operational within these biological matrices as shown in Fig. 3. The assay's limit of detection (LOD) was determined to be 0.17 nM in buffer, 5.1 nM in urine, and 23.9 nM in plasma. Nanozymes reduce cross-reactivity and matrix effects in assays due to their highly specific recognition sites, tailored to the target molecule during

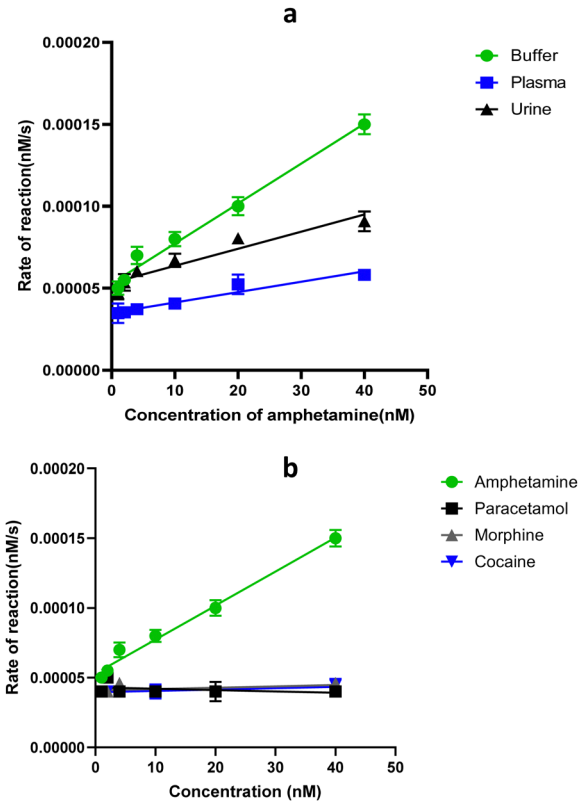

Fig. 4 Assay response to amphetamine in (a) buffer (5 mM PBS, pH 7.0), urine and plasma for the amphetamine range 0 to 40 nM. (b) Selectivity study against different drugs for the range 0.3 to 40 nM of amphetamine, paracetamol, morphine and cocaine. Assay conditions: each well contained 10 μL of the nanozyme MP11 (0.4 mg mL^{-1}), 135 μL of 10 nM BPR in PBS (5 mM, pH 7.0), 135 μL of H_2O_2 (50% w/v) and 20 μL of amphetamine solution (0, 0.3, 0.53, 0.6, 1, 2, 4, 10, 20, and 40 nM).

polymerization. These sites allow nanozymes to selectively bind the analyte, minimizing interference from other substances in biological samples. Unlike traditional ELISA assays, which often suffer from non-specific binding and matrix effects due to the complexity of samples like blood or urine, nanozymes offer enhanced selectivity. Nanozymes enable robust catalytic activity and more accurate detection in complex matrices, providing a stable and specific alternative to antibody-based assays.

Additionally, assay performance was measured over 6 months for Au/MIP nanozymes stored in fridge at 5 °C. No noticeable variations were observed for nanozymes stored in these conditions (data not shown), indicating excellent stability of synthesised materials. Additionally, the stability and performance of the nanozyme and the assay were assessed over the course of a year. The nanozyme was stored in solution at 4 °C in 5 mM PBS. It remained very stable with constant activity for the first 60 days. However, the assay response decreased by 6.7% after 90 days and by 13.3% after 180 days, after which the response stabilized. This decline is likely due to aggregation and biological contamination. Future studies will aim to improve storage conditions, such as lyophilization of the nanozyme and the use of preservatives like Proclin-200, as shown in Fig. S14 (ESI†).

The key advantage of the nanozyme assay presented here is the high selectivity. Additionally, nanozymes can be relatively easy to design and prepare with high yields. The nanozyme assay demonstrates superior sensitivity compared to other methods, with a remarkably low limit of detection (LOD) of 0.17 nM (0.023 ng mL^{-1}), which is orders of magnitude lower than other assays (Table 2). Its linearity range of 0.6–40 nM (0.08–5.41 ng mL^{-1}) is also highly precise, enabling accurate detection of very low amphetamine concentrations. This exceptional performance is achieved through the enhanced catalytic activity of the nanozyme, which benefits from the increased surface area of smaller gold nanoparticles. Additionally, the stability and specificity of the nanozyme assay further enhance its reliability, making it a highly effective tool for amphetamine detection and potentially applicable for different targets.

3. Conclusions

A novel method for synthesizing peroxidase-mimicking nanozymes using gold-core nanoparticles has been developed. This method involves a localized Fenton-like polymerization reaction on the surface of gold nanoparticles, performed in the presence of an immobilized target template. The resulting Au/MIP nanozymes were used in the colorimetric detection of amphetamine *via* BPR oxidation by hydrogen peroxide. This approach enables the effective detection of analytes in complex biological samples, offering a novel avenue for sensitive, specific, and user-friendly *in vitro* diagnostics. The developed Au/MIP nanozymes proved capable alternative of antibodies and enzymes in a homogeneous assay, as demonstrated in the detection of amphetamine within a concentration range of 0.6–40 nM (0.08–5.41 ng mL^{-1}). Compared to traditional methods, Au/MIP

Table 2 Performance comparison of amphetamine assays reported

Method	LOD (ng mL^{-1})	Linearity (ng mL^{-1})	Ref.
Colorimetric sensor	5.0×10^6	1×10^6–8×10^6	43
Solid gel colorimetric matrix	2.1×10^5	1×10^5–5×10^6	44
Au@Ag colorimetric biosensor	0.0149	0–0.1	45
Inorganic colorimetric assay	7.5×10^5	5×10^5–9×10^5	46
sDNAzyme assay	0.5	0–500	47
MIP-dye displacement assay	9.0×10^3	1×10^7–1×10^9	48
Hybrid nanozyme	28.6	0–100	49
Nanozyme assay	0.023 ng mL^{-1}, 0.17 nM	0.08–5.41 ng mL^{-1}, 0.6–40 nM	This study

nanozymes offer numerous advantages, including cost-effectiveness, robustness, a simple and generic preparation protocol, and convenient application in a homogeneous assay format that involves only a single step: addition of a test sample to a mixture of nanozyme, dye, and hydrogen peroxide. This measurement process doesn't necessitate further additions or washing steps and can be performed in a relatively short time (30 min). The application of Au/MIP nanozymes in homogeneous assays has been validated with real samples such as plasma and urine, showing recorded detection limits of 23.9 and 5.1 nM, respectively. We believe that the proposed Au/MIP nanozymes and their application in homogeneous assays have the potential to serve as a valuable alternative to ELISA and other popular *in vitro* diagnostic assays.

4. Methods

4.1 Synthesis of Au/MIP nanozymes

The preparation of the nanozyme was carried out by free radical polymerization using a solid phase, which comprises activation, salinization and immobilization of templates, and finally, polymerization to produce nanozyme. The preparation of glass beads was followed as described in the ESI.† For the solid phase synthesis, glass beads were functionalized with amphetamine. For that, 60 g of glass beads were incubated in amphetamine (65 mg, 0.481 μmol) in borate buffer (65 mL, 100 mM, pH 9.2) for 8 h, protected from light. In order to block unreacted iodine groups, mercaptoethanol (10 μL, 0.143 μmol) of was added to the mixture and incubated for 2 h. Subsequently, the glass beads were washed (100 mL × 2 times) with water and then acetone (100 mL × 4 times) and then dried under vacuum. The synthesis of Au/MIP nanozymes was performed as follows: each monomer was dissolved separately in PBS (1 mL, 100 mM, pH 7.5). *N*-3-Aminopropyl meth acrylamide (3 mg, 17 μmol), *N*-isopropyl acrylamide (19.5 mg, 172 μmol), *N*-*tert*-butyl acrylamide solution (400 μL, 236 μM in ethanol), acrylic acid (50 μL, 313 μM in water), *N*,*N*′-methylenebisacrylamide (400 μL, 38 μM in water) and 150 μL of gold nanoparticle stock solution (diameter 20 nm, 0.06 μm, OD) were mixed in PBS (50 mL, 5 mM PBS, pH 7.5). The monomeric solution was then sonicated for 20 min under nitrogen. 30 g of glass beads modified with amphetamine (template) were added to the monomeric solution. The polymerization was initiated *via* addition of hydrogen peroxide (50% w/v, 600 μL, 14.7 mM). The resulting mixture was shaken for 2 h during polymerization. The same steps were used to prepare a control polymer by replacing the amphetamine modified glass beads with blank glass beads (only silanized, with no amphetamine). Thus, the control polymer used was a non-imprinted polymer decorated with gold nanoparticles (AuNPs/NIP). After polymerization, the solution was discarded and the solid phase was transferred to a solid phase extraction (SPE) cartridge and washed with water at 4 °C (40 mL × 2 times). Then, the resulting Au/MIP nanozymes were eluted from the solid phase, first by washing with hot water (60 °C, 30 mL × 2 times) and then hot ethanol (60 °C, 30 mL × 2 times). Finally, the Au/MIP nanozymes were dialyzed (72 h), using a 10 kDa cut-off snake skin dialysis membrane and water was changed every 4 hours. Detailed information about chemicals is described in ESI.†

4.2 Transmission electron microscopy (TEM)

Continuous carbon film-coated 200 sq. copper TEM grids (Agar Scientific, UK) were used for the imaging. The grids were plasma glow-discharged in a Quorum Gloqube plus for 30 seconds at 30 mA to create a hydrophilic surface. An 8 μL droplet of 0.01% w/w aqueous 5 nm gold NP core -MIP dispersions were placed on the surface-treated grid for 5 min, and then excess dispersion was removed using filter paper. Then an 8 μL droplet of a 2% w/v aqueous solution of uranyl acetate (negative stain) was added to the sample-loaded grid for 1 min, and excess stain was removed using filter paper. The grid was dried using a vacuum hose and imagined was performed on a Joel JEM-1400 instrument at 120 kV equipped with an EMSIS Xarosa 20 mp digital camera with Radius software. The same method was used to prepare the grids for 20 nm, 50 nm and 100 nm, gold NP core -MIP dispersions.

4.3 Dynamic light scattering (DLS)

The size of the nanoparticles was determined using a Zetasizer Nano (Malvern Instruments Ltd, UK).

4.4 Development of the assay

Corning® 96-wells microplates (300 μL well volume) and a Hidex Sense 425–301 microplate reader were employed for measurements. Nanozyme catalytic activity was evaluated using the colorimetric assay format, measuring the absorbance change due to the oxidation of Bromo pyrogallol red (BPR, a chromogenic substrate) by hydrogen peroxide (H_2O_2), similar to other peroxidase-like activity assays.

4.5 Assay optimization, adjustment of BPR and pH

Different concentrations of BPR were tested (0.1 nM to 10 μM). A calibration plot was obtained by measuring the absorbance at 546 nm (Fig. S4, ESI†). A 10 nM BPR concentration was identified as the optimal concentration. During pH optimization, phosphate buffer (PBS, 5.0 mM, pH 7.4 at 25 °C) solution was used in the range between pH 6–8, while carbonate buffer (5.0 mM carbonate–bicarbonate buffer, pH 9.6 at 25 °C) was used for pH 9. For the assay development, each well contained 10 μL of the nanozyme (0.4 mg mL^{-1}), 135 μL of 10 nM BPR prepared with buffer range at pH 6–9, 135 μL of H_2O_2 (50% w/v) and 20 μL of 66.7 nM amphetamine.

4.6 Assay optimization, adjustment of nanozyme concentration

Each well contained 20 μL of amphetamine (66.7 nM), 10 μL of Au/MIP nanozymes in a concentration range of 0.2 to 0.6 mg mL^{-1}, 135 μL of BPR (10 nM) and 135 μL of H_2O_2 (50% w/v, 14.7 nM).

4.7 Assay optimization *via* hydrogen peroxide concentration adjustment

Each well contained 10 μL of Au/MIP nanozyme (0.4 mg mL^{-1}), 135 μL of BPR (10 nM). 20 μL of amphetamine (66.7 nM) and 135 μL of H_2O_2 (0.0 to 14.7 mM).

4.8 Assay optimization, adjustment of template concentration

Each well contained 10 μL of Au/MIP nanozyme (0.4 mg mL^{-1}), 135 μL of BPR (10 nM) and 135 μL of H_2O_2 (14.4 mM) with different concentrations of amphetamine (0.3 to 133 nM).

4.9 Optimisation of gold core size

To investigate the influence of AuNPs' size on the performance of the nanozyme assay, we employed the previously described solid-phase polymerization protocol. Different Au/MIP nanozymes were prepared by adding of Au nanoparticles (150 μL, 0.06 mM) with varying diameters (5, 20, 50, and 100 nm) to the polymeric mixture. The assay results revealed that Au/MIP nanozymes prepared with Au particles having a diameter of 5 nm exhibited significantly higher catalytic activity.

Ethics approval and consent to participate

Not applicable.

Consent for publication

Authors grant permission for the publication of research findings and related content, ensuring compliance with all ethical guidelines and copyright regulations.

Data availability

The data supporting this article have been included as part of the ESI.†

Conflicts of interest

SP and EP declare conflict of interest related to shareholding in MIP Discovery.

Acknowledgements

The authors express gratitude for the doctoral scholarship from Mustansiriyah University, College of Science, Chemistry Department, Baghdad, Iraq, awarded to S. H. A. Additionally, the authors gratefully acknowledge the University of Leicester Core Biotechnology Services Electron Microscopy Facility and Natalie S. Allcock for their support in producing TEM images of Au/MIP nanozymes.

References

1 H. Wei, G. Li and J. Li, *Biomedical Nanozymes: From Diagnostics to Therapeutics*, Springer Nature, 2023.
2 G. Sharma, S. Chatterjee, C. Chakraborty and J.-C. Kim, Advances in Nanozymes as a Paradigm for Viral Diagnostics and Therapy, *Pharmacol. Rev.*, 2023, **75**, 739–757.
3 B. Jiang, *et al.*, Standardized assays for determining the catalytic activity and kinetics of peroxidase-like nanozymes, *Nat. Protoc.*, 2018, **13**, 1506–1520.
4 X. Liu, *et al.*, Peroxidase-like activity of smart nanomaterials and their advanced application in colorimetric glucose biosensors, *Small*, 2019, **15**, 1900133.
5 G.-J. Cao, X. Jiang, H. Zhang, T. R. Croley and J.-J. Yin, Mimicking horseradish peroxidase and oxidase using ruthenium nanomaterials, *RSC Adv.*, 2017, **7**, 52210–52217.
6 C. Jiang, J. Zhu, Z. Li, J. Luo, J. Wang and Y. Sun, Chitosan–gold nanoparticles as peroxidase mimic and their application in glucose detection in serum, *RSC Adv.*, 2017, **7**, 44463–44469.
7 Q. Liu, A. Zhang, R. Wang, Q. Zhang and D. Cui, A review on metal-and metal oxide-based nanozymes: properties, mechanisms, and applications, *Nano-Micro Lett.*, 2021, **13**, 1–53.
8 N. Xu, S. Jin and L. Wang, Metal nanoparticles-based nanoplatforms for colorimetric sensing: A review, *Rev. Anal. Chem.*, 2021, **40**, 1–11.
9 J. Chen, *et al.*, Glucose-oxidase like catalytic mechanism of noble metal nanozymes, *Nat. Commun.*, 2021, **12**, 3375.
10 Y. Qin, Y. Ouyang and I. Willner, Nucleic acid-functionalized nanozymes and their applications, *Nanoscale*, 2023, **15**(35), 14301–14318.
11 X. Tao, X. Wang, B. Liu and J. Liu, Conjugation of antibodies and aptamers on nanozymes for developing biosensors, *Biosens. Bioelectron.*, 2020, **168**, 112537.
12 R. Yu, R. Wang, Z. Wang, Q. Zhu and Z. Dai, Applications of DNA-nanozyme-based sensors, *Analyst*, 2021, **146**, 1127–1141.
13 H. Cheng, *et al.*, Integrated nanozymes with nanoscale proximity for *in vivo* neurochemical monitoring in living brains, *Anal. Chem.*, 2016, **88**, 5489–5497.
14 L. Wang, L. Xiao, R.-Z. Zhang, L.-Z. Qiu, R. Zhang and H.-X. Shi, Effects of acrylate/acrylamide polymers on the adhesion, growth and differentiation of Muse cells, *Biomed. Mater.*, 2018, **14**, 015003.
15 Z. Zhang, X. Zhang, B. Liu and J. Liu, Molecular imprinting on inorganic nanozymes for hundred-fold enzyme specificity, *J. Am. Chem. Soc.*, 2017, **139**, 5412–5419.
16 Z. Zhang, B. Liu and J. Liu, Molecular imprinting for substrate selectivity and enhanced activity of enzyme mimics, *Small*, 2017, **13**, 1602730.
17 O. S. Ahmad, T. S. Bedwell, C. Esen, A. Garcia-Cruz and S. A. Piletsky, Molecularly imprinted polymers in electrochemical and optical sensors, *Trends Biotechnol.*, 2019, **37**, 294–309.
18 A. H. Safaryan, A. M. Smith, T. S. Bedwell, E. V. Piletska, F. Canfarotta and S. A. Piletsky, Optimisation of the preservation

conditions for molecularly imprinted polymer nanoparticles specific for trypsin, *Nanoscale Adv.*, 2019, **1**, 3709–3714.
19 A. G. Cruz, *et al.*, Design and fabrication of a smart sensor using in silico epitope mapping and electro-responsive imprinted polymer nanoparticles for determination of insulin levels in human plasma, *Biosens. Bioelectron.*, 2020, **169**, 112536.
20 A. Garcia-Cruz, O. Ahmad, K. Alanazi, E. Piletska and S. Piletsky, Generic sensor platform based on electro-responsive molecularly imprinted polymer nanoparticles (e-NanoMIPs), *Microsyst. Nanoeng.*, 2020, **6**, 83.
21 A. Garcia-Cruz, T. Cowen, A. Voorhaar, E. Piletska and S. A. Piletsky, Molecularly imprinted nanoparticles-based assay (mina)–detection of leukotrienes and insulin, *Analyst*, 2020, **145**, 4224–4232.
22 L. Gao, *et al.*, Intrinsic peroxidase-like activity of ferromagnetic nanoparticles, *Nat. Nanotechnol.*, 2007, **2**, 577–583.
23 Y. Jv, B. Li and R. Cao, Positively-charged gold nanoparticles as peroxidiase mimic and their application in hydrogen peroxide and glucose detection, *Chem. Commun.*, 2010, **46**, 8017–8019.
24 R. V. Shutov, *et al.*, Introducing MINA–the molecularly imprinted nanoparticle assay, *Small*, 2014, **10**, 1086–1089.
25 Y. García, J. Czulak, E. D. Pereira, S. A. Piletsky and E. Piletska, A magnetic molecularly imprinted nanoparticle assay (MINA) for detection of pepsin, *React. Funct. Polym.*, 2022, **170**, 105133.
26 S. Jimenez-Falcao, J. M. Méndez-Arriaga, V. García-Almodóvar, A. A. García-Valdivia and S. Gómez-Ruiz, Gold Nanozymes: Smart Hybrids with Outstanding Applications, *Catalysts*, 2022, **13**, 13.
27 J. Lou-Franco, B. Das, C. Elliott and C. Cao, Gold nanozymes: from concept to biomedical applications, *Nano-Micro Lett.*, 2021, **13**, 1–36.
28 Y. Lin, J. Ren and X. Qu, Catalytically active nanomaterials: a promising candidate for artificial enzymes, *Acc. Chem. Res.*, 2014, **47**, 1097–1105.
29 Y. Dai, S. Liu and N. Zheng, C_2H_2 treatment as a facile method to boost the catalysis of Pd nanoparticulate catalysts, *J. Am. Chem. Soc.*, 2014, **136**, 5583–5586.
30 S. Navalon, R. Martin, M. Alvaro and H. Garcia, Gold on diamond nanoparticles as a highly efficient Fenton catalyst, *Angew. Chem., Int. Ed.*, 2010, **49**, 8403–8407.
31 M. Zandieh and J. Liu, Nanozyme catalytic turnover and self-limited reactions, *ACS Nano*, 2021, **15**, 15645–15655.
32 Y. Yang, *et al.*, Challenges in radical/nonradical-based advanced oxidation processes for carbon recycling, *Chem Catal.*, 2022, **2**, 1858–1869.
33 F. Canfarotta, A. Poma, A. Guerreiro and S. Piletsky, Solid-phase synthesis of molecularly imprinted nanoparticles, *Nat. Protoc.*, 2016, **11**, 443–455.
34 K. Smolinska-Kempisty, A. Guerreiro, F. Canfarotta, C. Cáceres, M. J. Whitcombe and S. Piletsky, A comparison of the performance of molecularly imprinted polymer nanoparticles for small molecule targets and antibodies in the ELISA format, *Sci. Rep.*, 2016, **6**, 37638.
35 P. X. Medina Rangel, *et al.*, Solid-phase synthesis of molecularly imprinted polymer nanolabels: Affinity tools for cellular bioimaging of glycans, *Sci. Rep.*, 2019, **9**, 3923.
36 K. Haupt, P. X. Medina Rangel and B. T. S. Bui, Molecularly imprinted polymers: Antibody mimics for bioimaging and therapy, *Chem. Rev.*, 2020, **120**, 9554–9582.
37 M. Drozd, M. Pietrzak, J. Pytlos and E. Malinowska, Revisiting catechol derivatives as robust chromogenic hydrogen donors working in alkaline media for peroxidase mimetics, *Anal. Chim. Acta*, 2016, **948**, 80–89.
38 F. Paul and T. R. Weikl, How to distinguish conformational selection and induced fit based on chemical relaxation rates, *PLoS Comput. Biol.*, 2016, **12**, e1005067.
39 J. Li, W. Liu, X. Wu and X. Gao, Mechanism of pH-switchable peroxidase and catalase-like activities of gold, silver, platinum and palladium, *Biomaterials*, 2015, **48**, 37–44.
40 Drugs UNOo, Laboratory C, Section S. *Recommended Methods for the Identification and Analysis of Amphetamine, Methamphetamine and Their Ring-substituted Analogues in Seized Materials: Manual for Use by National Drug Testing Laboratories*. New York: United Nations (2006).
41 K. E. Moeller, J. C. Kissack, R. S. Atayee and K. C. Lee, Clinical interpretation of urine drug tests: what clinicians need to know about urine drug screens, *Mayo Clinic Proceedings*, Elsevier, 2017.
42 R. S. Matson, Interference in ELISA, *ELISA: Methods and Protocols*, Springer, 2023.
43 A. Argente-García, N. Jornet-Martínez, R. Herráez-Hernández and P. Campíns-Falcó, A solid colorimetric sensor for the analysis of amphetamine-like street samples, *Anal. Chim. Acta*, 2016, **943**, 123–130.
44 A. Choodum, P. Kanatharana, W. Wongniramaikul and N. NicDaeid, A sol–gel colorimetric sensor for methamphetamine detection, *Sens. Actuators, B*, 2015, **215**, 553–560.
45 K. Mao, Z. Yang, J. Li, X. Zhou, X. Li and J. Hu, A novel colorimetric biosensor based on non-aggregated Au@Ag core–shell nanoparticles for methamphetamine and cocaine detection, *Talanta*, 2017, **175**, 338–346.
46 S. T. Krauss, *et al.*, Objective method for presumptive field-testing of illicit drug possession using centrifugal microdevices and smartphone analysis, *Anal. Chem.*, 2016, **88**, 8689–8697.
47 K. Mao, Z. Yang, P. Du, Z. Xu, Z. Wang and X. Li, G-quadruplex–hemin DNAzyme molecular beacon probe for the detection of methamphetamine, *RSC Adv.*, 2016, **6**, 62754–62759.
48 J. W. Lowdon, *et al.*, A molecularly imprinted polymer-based dye displacement assay for the rapid visual detection of amphetamine in urine, *Molecules*, 2020, **25**, 5222.
49 O. Adegoke, S. Zolotovskaya, A. Abdolvand and N. N. Daeid, Biomimetic graphene oxide-cationic multi-shaped gold nanoparticle-hemin hybrid nanozyme: Tuning enhanced catalytic activity for the rapid colorimetric apta-biosensing of amphetamine-type stimulants, *Talanta*, 2020, **216**, 120990.